

# Impurity effects in coaxial-connector photonic crystals: A quasi-one-dimensional periodic system

Ranjit D. Pradhan

*Applied Optics Center of Delaware, Delaware State University, Dover, Delaware 19901*

George H. Watson

*Department of Physics and Astronomy, University of Delaware, Newark, Delaware 19716*

(Received 11 December 1998)

A one-dimensional coaxial connector photonic crystal has constructed from a series of standard high frequency coaxial cable “tee” and “barrel” connectors, forming a quasi-one-dimensional periodic system with periodicities comparable to microwave wavelengths. At the appropriate frequencies, “Bragg-like” reflections of the gigahertz-frequency sinusoidal signals from the open ends of the tee connectors result in the formation of stop bands for which transmission of signals at these frequencies is forbidden. Changing the amplitude or/and phase of these reflections is analogous to the introduction of defects (impurities) in the periodic structure and is evidenced by appearance of impurity peaks of enhanced transmission in the stop bands. This system readily allows fixing of the defect location within a unit cell to one particular configuration. It also allows a direct control over the location of defects relative to each other. By using this system a wide variety of impurity-induced effects in photonic crystals such as surface effects, inter-impurity interactions, and stop band widening have been demonstrated. [S0163-1829(99)06027-0]

## I. INTRODUCTION

Periodicity in a dielectric medium can have a profound effect on the electromagnetic waves that propagate through it. The so-called photonic crystal can forbid photon transport for certain bands of frequencies irrespective of polarization or propagation direction, leading to a complete photonic band gap (PBG).<sup>1,2</sup> Such photonic crystals are anticipated to have a significant technological impact on a wide range of photonic applications.<sup>3</sup> The application of photonic crystals will be enhanced by “doping” them with defects/impurities to generate defect/impurity states.<sup>4–6</sup> Impurity effects are extremely sensitive to the configuration of the impurities in their respective unit cells, as seen in previous studies where the donor impurity levels split on displacement of the donor impurity relative to its lattice site.<sup>4</sup> As the impurities begin to approach within a characteristic length of each other, these effects are also determined by the relative positions of neighboring impurity sites; impurity modes were found to be dependent on whether the defects appeared on neighboring lattice sites or were separated by a lattice site.<sup>7</sup>

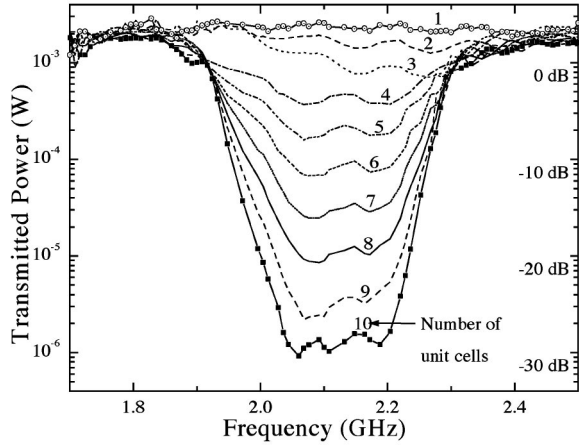
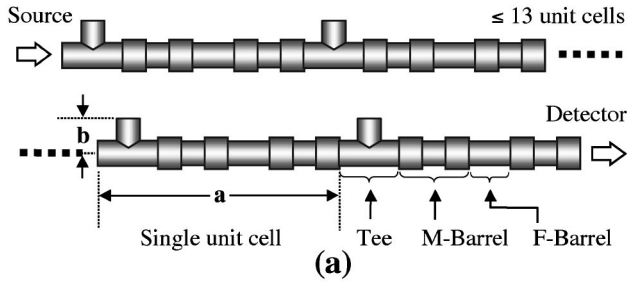
The coaxial connector photonic crystal (CCPC) used in this study is constructed out of a series of “tee” and “barrel” connectors (standard  $N$ -type high frequency coaxial cable connectors) to form a quasi-one-dimensional (1D) periodic system, as shown in Fig. 1(a). The open ends of the tee connectors reflect microwave frequency signals. The spatial period  $a$  and the height  $b$  of the tees are parameters that characterize this periodic system and are comparable to microwave wavelengths (frequency  $\sim$  GHz). Thus within the appropriate band of frequencies, a “Bragg-like” constructive interference of the signals in the backward direction results in the formation of stop bands in the transmission spectrum. Introduction of a defect into the CCPC perturbs the amplitude and/or phase of the reflected signal from the open end of a tee. The CCPC is a system which fixes the defect location within a unit cell to one particular configuration and allows a direct control over the location of defects relative to

each other. Another advantage is that the CCPC may be assembled from off-the-shelf components.

In previous work we reported on impurity effects in polystyrene colloidal photonic crystals.<sup>8,9</sup> Dopants of a different particle size or material were substitutionally introduced into a host matrix of polystyrene microspheres; broad impurity states arose in the stop band as a result of the doping. Owing to the small deviations in the host and dopant polystyrene microsphere diameters, the impurity effects in the doped colloidal crystal system represented an average over various configurations of defects slightly displaced from their mean position in the unit cell. Moreover, being a self-assembling system, there was no precise control over the configurations of the defect site arrangements relative to each other. Thus the ability to isolate a particular configuration with a well-defined position of the impurity “atom” within the fcc unit cell was not possible. There was also no way of arranging the defects in a particular way relative to one another. The CCPC system allowed us to overcome these limitations and replicate some of the impurity effects previously observed in doped colloidal photonic crystals.

## II. EXPERIMENTAL DETAILS

The CCPC shown in Fig. 1(a) was based on components that are generically termed “ $N$ -connectors”<sup>10</sup> and had a characteristic impedance of  $50\Omega$  in the 100-MHz–20-GHz range. Connecting these elements as shown in Fig. 1(a) yielded a periodic system with the spatial period ( $a=12.05$  cm) and the height of the tees ( $b=2.35$  cm) characterizing its periodicity. Impurities were introduced at tee sites in the CCPC by changing the amplitude and/or phase of the signals reflected from the open end of the tee. The types of doping performed on the CCPC samples is shown in Fig. 2(a). Defects consisting of different combinations of connectors and terminators had different dopant “strengths” and were used



(b)

FIG. 1. (a) The coaxial connector photonic crystal (CCPC) is a quasi-one-dimensional periodic system made up of a series of standard high frequency coaxial cable connectors. The “tee” connectors have three female ends, the  $M$  barrels have two male ends, and the  $F$  barrels have two female ends. The unit cell length  $a$  and the height  $b$  of the tees are parameters that characterize this periodic system. The maximum number of unit cells in this study was 13. (b) The transmission spectra through the CCPC are shown for various number of unit cells (indicated above each curve). The transmitted power shown is normalized to the transmitted power through a coaxial cable (non-periodic structure). The spectra show a stop band centered at  $\sim 2.10$  GHz. Within the stop band an attenuation of over three orders of magnitude is observed for 10 or more unit cells. The stop band width is about 10% of the center frequency.

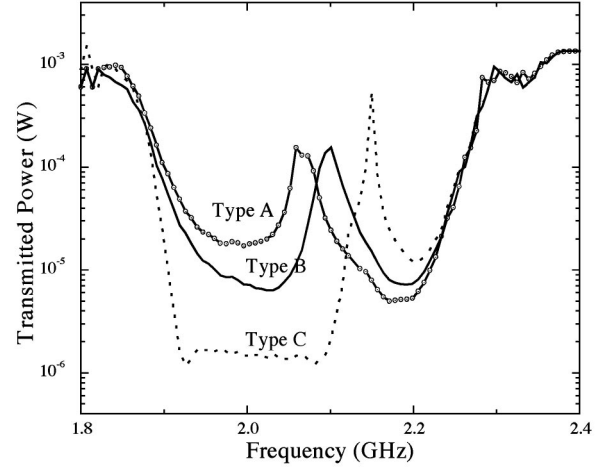
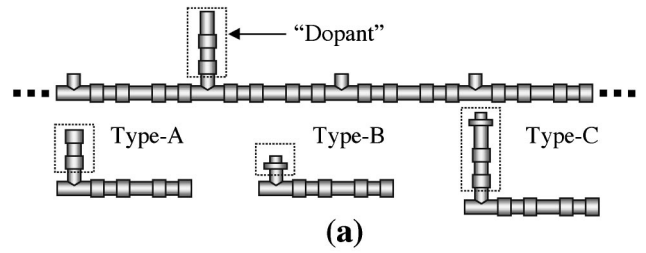
to perturb the reflected signal from a specific defect site.

The transmission through the CCPC was measured at microwave frequencies (100 MHz–20 GHz), generated with a Hewlett-Packard HP83620A synthesized continuous wave (c.w.) generator. The c.w. signals were modulated (square wave amplitude modulation) at a frequency of 1 KHz using a Hewlett-Packard HP11720A pulse modulator to facilitate detection using standard lock-in detection techniques. The detector used was a Hewlett-Packard HP423B, 10-MHz–12.4-GHz, low-barrier Schottky diode detector with an input impedance of  $50 \Omega$ . The transmission spectra through the CCPC were normalized with those measured through a coaxial cable (continuous nonperiodic system) to account for any nonuniform spectral response of the source, pulse modulator, and detection system.

### III. DISCUSSION OF THE RESULTS

#### A. “Undoped” crystal

Figure 1(b) shows the transmission spectra through an undoped CCPC. This figure shows a stop band opening at a



(b)

FIG. 2. (a) A doped CCPC: Introducing a defect/impurity in the CCPC of Fig. 1(a) can be achieved by “capping” the open end of the tee with a combination of connectors and terminators as shown at the top of (a). Various combinations that may be used to generate dopants (defects) with different “strengths” are shown. Defect type A is a  $M$  barrel connected to the open end of the tee. Type B is a BNC adaptor and type C is a combination of an  $M$  barrel,  $F$  barrel, and BNC adaptor. (b) Transmission spectra for a doped CCPC: Defect states or regions of enhanced transmission appear within the stop band on introduction of the defects shown above. Changing the defect type changes the defect strength and shifts the defect-state location within the stop band.

frequency  $f_0 = 2.10$  GHz. The typical bandwidth is 10% of the center frequency. In the case of typical polystyrene colloidal crystals the stop band width is typically less than 3% for the undoped crystals and less than 5% for the doped crystals.<sup>8</sup> For the  $N$  connectors the phase speed is  $2/3$  the speed of light in vacuum. On using the Bragg law, one finds that the spatial period  $a = 12.05$  cm alone does not determine the characteristic period. Instead the stop band center frequency is very sensitive to the height  $b$  of the tee connectors that introduce the scattering. This was determined by varying the height of the “tees” using  $M$ - and  $F$ -barrel connectors. However, use of the parameter  $b$  does not yield the center frequency of 2.10 GHz observed in the transmission spectra. For example, in the structure of Fig. 1(a),  $b = 2.35$  cm. The Bragg law is expressed as

$$f_0 = m \frac{v}{2\tilde{a}},$$

where  $\tilde{a}$  is the characteristic period. With  $\tilde{a} = b = 2.35$  cm, we get the first order ( $m = 1$ ) stop band frequency  $f_0 \approx 4.26$

GHz. On the other hand,  $\tilde{a}=a=12.05$  cm yields  $f_0\approx 0.83$  GHz. The observed first order stop band center frequency is at  $f_0=2.10$  GHz. The characteristic period for the 1D system of Fig. 1(a) lies between the two parameters  $a$  and  $b$ . In all other respects this system behaves like a 1D system as the following discussion suggests. Thus it is appropriate to call this system a *quasi 1D periodic system*. Figure 1(b) shows the transmission spectra with an increasing number of unit cells. The number of unit cells is indicated at the bottom of the individual curves. It is interesting to note that the transmission spectrum for a single unit cell is “flat.” Had the interference effects within a single tee connector been significant there would have been sufficient attenuation from a single unit cell in a manner analogous to a single layer reflection coating. Instead the optical stop band formation begins only after about three unit cells indicating a partial coherent addition of components reflected from different tees in this quasi-1D system. The attenuation of transmitted signals in the stop band rapidly increases with number of unit cells with a  $-3$  dB attenuation per unit cell.

### B. “Doped” crystal

The introduction of impurities of the types indicated in Fig. 2(a) significantly alters the internal details of the stop bands. As in the case of the colloidal crystals, impurity effects manifest themselves by the appearance of impurity modes in the stop bands. The details of the transmission spectrum around the first order stop band is shown in Fig. 2(b) for a crystal with 10 unit cells. The transmitted power at the frequencies of these impurity modes rose by at least an order of magnitude relative to the stop band “floor.” The transmission spectra, shown here for the doped CCPC, are those for the defect types A, B, and C shown in Fig. 2(a). The defect type A is a male-male  $N$  connector connected to the free end of the tee connectors in the periodic system. Type B is a male  $N$ -to-BNC adapter and type C is a series combination of a male-male  $N$  connector, a female-female  $N$  connector, and a male  $N$ -to-BNC adapter. These three defects of different dopant “strengths” resulted in an impurity peak at a different position within the stop band, allowing for the tunability of the defect mode frequency.

### C. Investigation of “surface effects”

In solid state systems the surface plays an important role since the surface atoms reside in a vastly different environment from those in the bulk.<sup>11</sup> We observed the effects of the “surface” (end effects) in the coaxial connector crystal as well. For example, if the impurity was located on the first unit cell near the source, the transmission properties of a doped crystal with  $N$  unit cells were difficult to distinguish from those for an undoped crystal with  $(N-1)$  unit cells. A similar phenomenon occurred when the impurity was located close to the detector. These results are summarized in Fig. 3. The inset shows the frequency range covering the entire stop band for a 1D coaxial crystal with 13 unit cells. The dotted curve in the inset is the transmission through an undoped crystal while the solid curve is for a single impurity at the center of the crystal. The main graph in Fig. 3 shows a magnified section of the region indicated in the inset. The various impurity modes shown in Fig. 3 are for different locations of

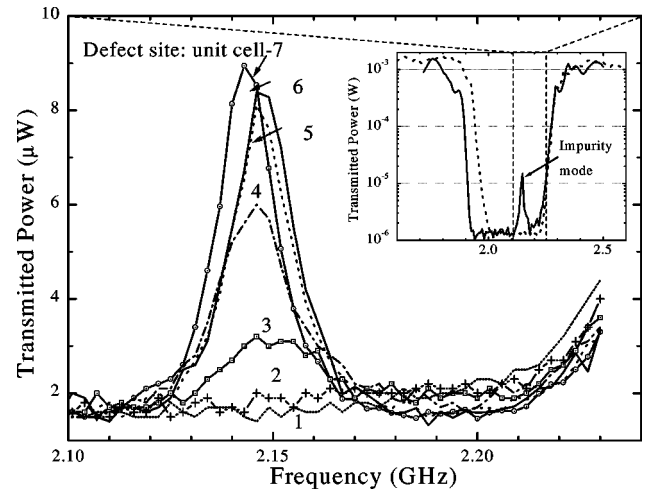


FIG. 3. Investigation of “surface” effects: This graph shows the effect of varying the site of a single defect [type C in Fig. 2(a)] in a 13-unit cell CCPC. The inset shows the entire transmission spectrum from 1.6 to 2.6 GHz. The region around the impurity mode in the inset is magnified outside the inset. When the defect is located on the “surface” close to the source or the detector, the transmission spectra for the doped and the undoped CCPC are almost identical. As the defect site is moved to the interior of the crystal from unit cell 1, the height of the impurity modes increases and reaches a maximum at unit cell 7.

a single defect within the 13 unit cell crystal. The position of the unit cell (1 through 7) carrying the defect is also indicated. When the defect was located close to the source (input “surface”) on the first tee there were no signs of impurity effects within the stop band and the spectrum appeared similar to the undoped case. However, as the position of this single defect was moved inward, the height of the impurity peak rose and reached a maximum when the defect was located “deep” inside the crystal. Impurity peaks appeared similar if the defect position was not within the first 3–4 unit cells from the surface. The following sections deal with additional effects resulting from introduction of impurities. In all subsequent studies, care was exercised to avoid the above-mentioned surface effects.

### D. Effect of interaction between defects

Figure 4 shows a magnified region of the transmission spectrum containing the impurity modes with two impurities in a 13 unit cell crystal. The separation between the two impurity positions ( $\Delta$ ) are indicated besides the curves in units of  $a$ . Thus  $\Delta=1$  implies defects introduced in neighboring lattice sites. The curve with  $\Delta=6$  is for the case where the two defects were well separated (one each on unit-cells 4 and 10 from the source). In the  $\Delta=6$  case the impurity mode appeared at the same frequency ( $\sim 2.15$  GHz) as the impurity mode resulting from a single defect (see the inset of Fig. 3). However the transmission coefficient at the impurity mode was nearly an order of magnitude greater than that in the single impurity case.

The separation between the two defects was systematically reduced from  $\Delta=6$  to  $\Delta=1$ . The transmission spectra at the impurity modes changed dramatically with reduction in the separation  $\Delta$ . As the defects approached each other,

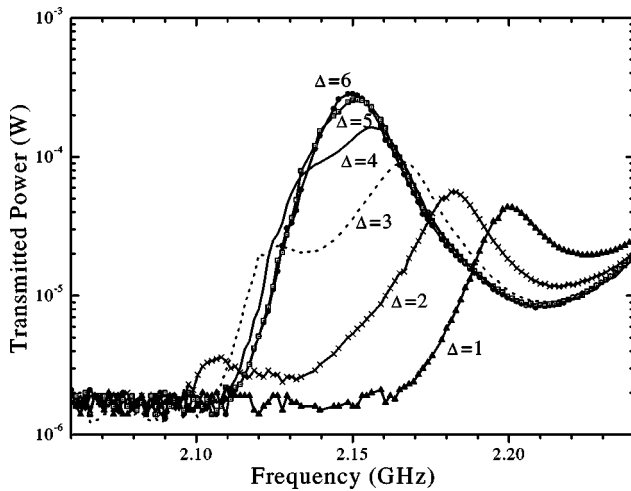


FIG. 4. Two defects: The stop band transmission spectra of impurity peaks are shown for a 13 unit cell CCPC doped with two defects. The defects are located at two sites separated by a distance  $\Delta$  (in units of  $a$ ).  $\Delta=1$  represents the case of neighboring defects while  $\Delta=6$  represents the case of two defects in unit cells 4 and 10 from the source. For the  $\Delta=6$  case the impurity peak is at the same frequency as the single impurity peak (see inset of Fig. 3) but is an order of magnitude higher. As the separation between the defects is reduced from  $\Delta=6$  to  $\Delta=1$  this impurity peak splits into two peaks with their frequency separation increasing with decreasing  $\Delta$ .

the impurity peak split into two distinct peaks. This can be seen more clearly for the cases where  $\Delta=2$  and 3. With reducing  $\Delta$ , the two distinct modes separated further. This indicates a strong interaction between the impurity modes. Two well separated defects create an impurity mode which is, in a sense, a summing of their individual effects. However, two closely spaced defects constitute an entirely different entity with a different impurity “strength.”

The effects of multiple impurities became even more pronounced with three defects introduced in the structure. Three defects also permitted comparison of the result of doping these structures with periodic or nonperiodic defects. Figure 5 shows the transmission spectra through a 13 unit cell structure with three defects. The two values of  $\Delta$  indicated for these curves indicates the separation between defects 1 and 2 and defects 2 and 3 respectively. If these two separations are equal the defects are arranged periodically. With the three defects well separated ( $\Delta=4,4$ ), the transmission coefficient at the resulting impurity mode was higher than the corresponding one and two defect cases. As in the crystal with two defects, the impurity peak separated into multiple modes as the impurities spatially approach each other. In the crystal with three defects, the impurity peak separated into three modes. This can be seen very clearly for the case with  $\Delta=2, 2$ . This separation into multiple impurity peaks occurred even if the defects were not arranged periodically as can be seen in the curves labeled  $\Delta=3, 2$  and  $\Delta=2, 3$ .

### E. Impurity-induced stop band widening

In earlier work on impurities in colloidal crystals it was observed that the optical stop bands displayed significant widening on introduction of impurities.<sup>8</sup> The widening was unsymmetrical with the high energy edge remaining rela-

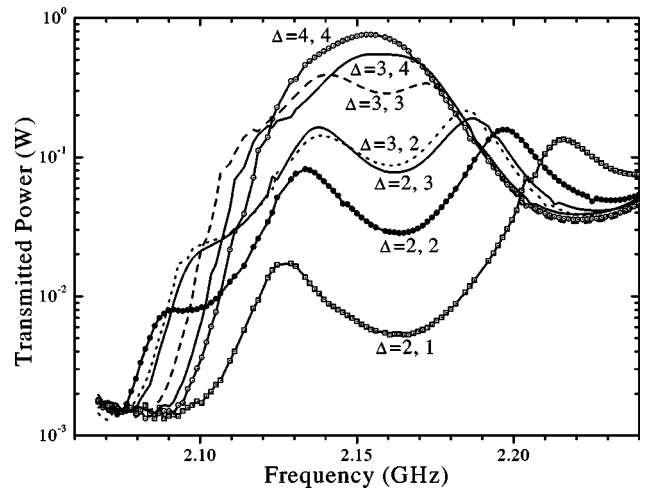


FIG. 5. Three defects: The stop band transmission spectra of impurity peaks are shown for a 13 unit cell CCPC doped with three defects. The two values of  $\Delta$  indicated for each curve are the separation for defects 1 and 2 and that for defects 2 and 3. For the case of well-separated defects ( $\Delta=4,4$ ) the impurity peak appears at the same frequency as the single and double impurity cases but its height is higher than both cases. As the separation between the defects is reduced the impurity peak splits into three individual peaks which further separate with decreasing  $\Delta$ . This splitting occurs for both the periodic (equal  $\Delta$ ) and nonperiodic (unequal  $\Delta$ ) impurity cases.

tively immune to the effects of band widening. One of the motivations behind this study of the CPCC was to check on the possible universality of such effects.

The CPCC displayed considerable widening of the stop bands on introduction of impurities, as seen in Fig. 6. The dashed curve in the figure is the transmission spectrum for an

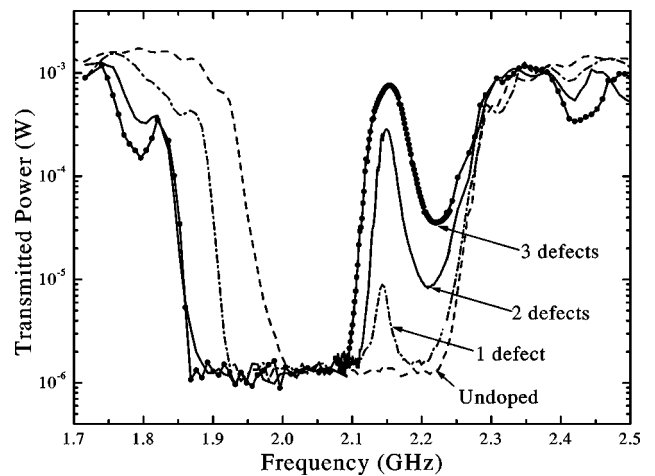


FIG. 6. Defects and band widening: The transmission spectra shown above are for a 13 unit cell crystal with increasing number (concentration) of defect sites from 0 (undoped) to 3. With increasing defect concentration the height of the impurity peak increases with a corresponding increase in the impurity peak width. For all concentrations the impurity peak frequency remains unchanged. On introduction of impurities, considerable stop band widening occurs and increases with increasing defect concentration. The stop band widening appears to occur towards the lower energy edge (valence band edge) of the stop band.

undoped crystal with 13 unit cells. The corresponding transmission curves for the crystals with 1, 2, and 3 defects are indicated. In the doped crystals, the defects were well separated to minimize their mutual interactions described earlier. Note that the frequency of the impurity modes remained fixed but the amplitude increased with increasing number of impurities. The width of the impurity peak also increased and the stop band widened. This increase in width was not indefinite but saturated at some point. The increase in the width of the stop band was observed to be as large as 40% of the undoped stop band width. This band widening is also unsymmetrical with the high energy or the conduction band edge remaining immobile; the widening is almost entirely towards the lower energy side or the valance band edge.

### F. A coaxial connector photonic crystal superlattice

Figure 7(a) shows a different periodic arrangement of the tees. It consists of a crystal consisting of 14 tees. The tees are grouped into pairs forming a single unit cell as shown in the figure; seven such unit cells form the “superlattice.” A single defect is introduced in this structure at the center and the transmission spectrum is compared with that for a regular crystal with 13 unit cells. The comparison of these two crystals is shown in Fig. 7(b). The undoped cases for both the regular crystal and the superlattice show that a noticeable band widening occurs with the introduction of the superlattice. On doping these two types of crystals, impurity modes occur in the stop bands. In both cases the stop bands are wider than the corresponding undoped cases. Again, the band widening is unsymmetrical and on the lower energy side.

## IV. SUMMARY

The effects of introducing defects in a periodic coaxial structure displayed the same general trends seen in previous work on doped polystyrene colloidal crystals. These effects included the appearance of impurity modes in the stop bands and unsymmetrical band widening. This quasi-one-dimensional system yielded stop band widths which were typically 10% of the center frequency with an attenuation of over three orders of magnitude in the transmission coefficient in a crystal with ten or more unit cells. With the introduction of impurities, the transmission coefficient rose at least an order of magnitude above the stop band floor. Reduction of the inter-impurity spacing led to splitting of the impurity modes and formation of an impurity band. A similar effect occurs in degenerate semiconductors leading to the formation of impurity bands which may overlap either the conduction or the valance band edges.<sup>12</sup> This easily realizable system can thus be used to reveal invaluable insights

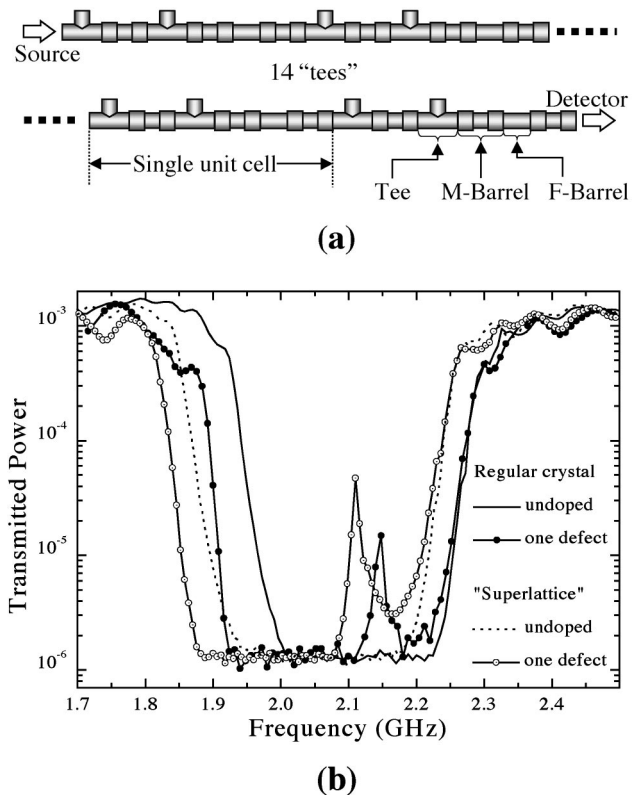


FIG. 7. Superlattice: (a) A CCPC superlattice is constructed by grouping two tee-connectors in a single unit cell as shown. Seven such unit cells form the superlattice with a total of 14 tees. A single defect was introduced at the center of the crystal. (b) Transmission spectra for the undoped and doped CCPC superlattice (14 tees) are compared with the corresponding cases for a regular CCPC with 13 unit cells. The undoped stop band width for the superlattice is greater than that for a regular crystal. The superlattice shows a higher impurity peak height and width and its stop band widens towards the valance band edge as seen in the case of the regular CCPC.

into some of the photonic band structure effects seen in previous work on doped polystyrene colloidal photonic crystals.

## ACKNOWLEDGMENTS

We would like to thank Dr. Vivek Agrawal, Toralf Bork, and Dr. Yanusz Murakowski, from Dr. Dan Van de Weide's group in the Department of Electrical Engineering, University of Delaware, for assistance with their Hewlett-Packard 100MHz-20GHz synthesized generators and for their helpful discussions. We would like to thank John A. Bloodgood for his work on this project during the initial stages. This work was supported by the National Science Foundation under Grant No. DMR-9510460.

<sup>1</sup>Special review issues: C. M. Bowden, J. P. Dowling, and H. O. Everitt, *J. Opt. Soc. Am. B* **10** (1993); G. Kurizki and J. W. Haus, *J. Mod. Opt.* **41** (1994).

<sup>2</sup>For a recent review see *Photonic Band Gap Materials*, edited by C. M. Soukoulis (Kluwer Academic Publishers, Dordrecht, 1996).

<sup>3</sup>E. Yablonovitch, *J. Mod. Opt.* **41**, 173 (1994).

<sup>4</sup>E. Yablonovitch, T. J. Gmitter, R. D. Meade, A. M. Rappe, K. D. Brommer, and J. D. Joannopoulos, *Phys. Rev. Lett.* **67**, 3380 (1991).

<sup>5</sup>S. L. McCall, P. M. Platzman, R. Dalichaouch, D. Smith, and S. Schultz, *Phys. Rev. Lett.* **67**, 2017 (1991).

- <sup>6</sup>K. M. Leung, J. Opt. Soc. Am. B **10**, 303 (1993).
- <sup>7</sup>M. Sigalas, C. M. Soukoulis, E. N. Economou, C. T. Chan, and K. M. Ho, Phys. Rev. B **48**, 14 121 (1993).
- <sup>8</sup>R. D. Pradhan, I. I. Tarhan, and G. H. Watson, Phys. Rev. B **54**, 13 721 (1996).
- <sup>9</sup>B. T. Rosner, G. Schneider, and G. H. Watson, J. Opt. Soc. Am. B **15**, 2654 (1998).
- <sup>10</sup>The various  $N$  connectors used in this setup were obtained from Pasternack Enterprises, P. O. Box 16759, Irvine, CA 92623 U.S.A. The tee connectors used had three female ends, the  $M$  barrels had two male ends, and the  $F$  barrels had two female ends.
- <sup>11</sup>C. Kittel, *Introduction to Solid State Physics* (Wiley, New York, 1996), 7th ed.
- <sup>12</sup>B. G. Streetman, *Solid State Electronic Devices* (Prentice-Hall, Englewood Cliffs, NJ, 1990).